

Design and analysis of dual-mode structure repetitive control based hybrid current regulation scheme for active power filters

Zou Zhixiang Wang Zheng Cheng Ming

(School of Electrical Engineering, Southeast University, Nanjing 210096, China)

Abstract: An all-digital hybrid current regulation scheme for the single-phase shunt active power filter (APF) is presented. The proposed hybrid current control scheme integrates the deadbeat control and the dual-mode structure repetitive control (DMRC) so that it can offer superior steady-state performance and good transient features. Unlike the conventional schemes, the proposed scheme-based APF can compensate both the odd and the even order harmonics in grid. The detailed design criteria and the stability analysis of the proposed hybrid current controller are presented. Moreover, an improved structure which incorporates the proposed hybrid controller and the resonant controller for tracking specific order harmonics is given. The relationships between the resonant controller and different repetitive control schemes are discussed. Experimental results verify the effectiveness and advantages of the proposed hybrid control scheme.

Key words: active power filter; dual-mode structure repetitive control (DMRC); current control; harmonic compensation; resonant controller

doi: 10.3969/j.issn.1003-7985.2013.04.010

With the increasing use of nonlinear loads in power systems and more strict requirements by grid codes, the power quality becomes a critical issue today. The nonlinear loads may cause significant low order harmonics, which will not only increase the power loss in distribution lines but also disturb some sensitive electric equipment. Both the passive and the active power filters (APF) have been proposed to alleviate such low order harmonics^[1-3]. Compared with the passive power filters, the APF is considered more attractive due to its high efficiency and controllability^[4]. The function of the APF is to generate the out-of-phase harmonics purposely to com-

pensate the existent harmonics in grid. In the past several years, the most important research line for the APF is related with the control schemes, which can effectively improve the performance of the APF system. In fact, the performance of the APF is mainly dependent on the current tracking capability. Many conventional current regulations, such as proportional integral (PI) control^[5], hysteresis control^[6] and deadbeat control^[7], etc. have been applied in the APF system. However, these solutions exhibit some well-known drawbacks^[8] and from the investigation of the experimental results, the current tracking capabilities based on these methods are relatively weak.

The repetitive control is another promising current regulation scheme today. Originating from the internal model principle, the repetitive control provides a high-performance solution for the grid current quality applications^[9-12]. The periodic disturbance and error can be easily eliminated by using this repetitive controller. Therefore, the repetitive controller can precisely track the reference current with various order harmonics, and it is very suitable for the current control in the APF application. However, the transient performance of the conventional repetitive controller is unsatisfactory for the APF application because the control output values update every N sample intervals and the error convergence rate is slow. N is the sampling times in a fundamental cycle. To accelerate the convergence rate, the odd-harmonic repetitive control scheme was proposed^[13]. Compared with the conventional repetitive controller, the odd-harmonic repetitive controller updates its output values every $N/2$ sample intervals, and the convergence rate is faster. Since the main harmonics in the power electronic system are odd harmonics, the odd-harmonic repetitive control (OHRC) was proposed for the shunt APF in Ref. [14]. In addition to the similar ability of harmonic rejection as the conventional repetitive control, the OHRC is verified to offer better transient performance. However, the OHRC only provides high gains for the odd harmonics but it has less controllability for the even order harmonics. Actually, the power system produces even order harmonics when power converters are employed under some unusual conditions^[15-16]. Unlike the OHRC, the dual-mode structure repetitive controller (DMRC) can eliminate both the odd and even harmonics^[17]. In addition, the DMRC also updates the control

Received 2013-06-12.

Biographies: Zou Zhixiang (1985—), male, graduate; Wang Zheng (corresponding author), male, doctor, associate professor, zzwang@seu.edu.cn.

Foundation items: The National Basic Research Program of China (973 Program) (No. 2013CB035603), the National Natural Science Foundation of China (No. 51007008, 51137001), the Ph. D. Programs Foundation of Ministry of Education of China (No. 20100092120043), the Fundamental Research Funds for the Central Universities.

Citation: Zou Zhixiang, Wang Zheng, Cheng Ming. Design and analysis of a dual-mode structure repetitive control based hybrid current regulation scheme for active power filters[J]. Journal of Southeast University (English Edition), 2013, 29(4): 407 – 413. [doi: 10.3969/j.issn.1003-7985.2013.04.010]

output values every $N/2$ sample intervals. Thus, the DMRC can not only improve the performance of grid current control under general current harmonic conditions, but also maintain the fast convergence rate. It should be noted that the dynamic performance of repetitive control is not satisfactory because of the memory cells in the forward channel. Therefore, the repetitive controller is usually improved by integrating a feedback controller^[18]. To provide good performance for both the steady-state and the transient operation of the APF, a novel hybrid current controller is proposed in this paper by integrating the deadbeat control and the DMRC. By using the proposed hybrid current controller, not only the advantages of the deadbeat controller, namely the fast transient response and easy digital implementation are maintained, but also the high robustness and accurate current tracking ability are provided.

1 System Description

Fig. 1 shows the system configuration, where a single-phase voltage source inverter (VSI) fed shunt APF is used to compensate the low order harmonics generated by a diode rectifier. The VSI fed APF is connected to the grid via an inductor. The diode rectifier feeds the paralleled capacitor and resistor load in the DC side. In this figure, E , V_c , i_L , i_c and i_{ref} are the grid voltage, the DC-link voltage, the load current, the compensation current and the reference current, respectively. \bar{p} and \bar{q} are the DC components of the instantaneous active and reactive power, respectively, and p_{loss} corresponds to the loss of the APF.

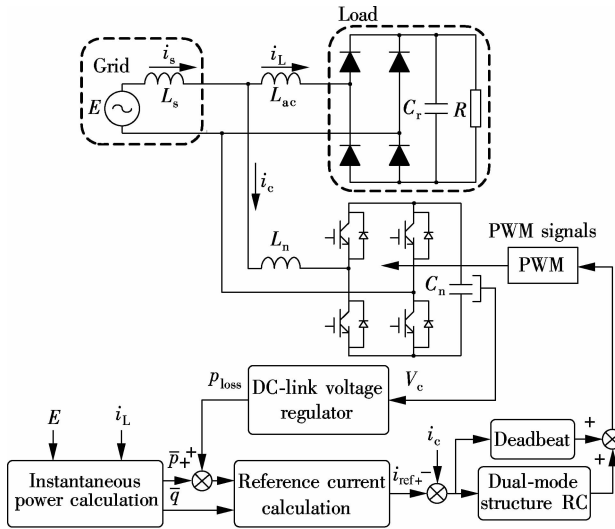


Fig. 1 System configuration of the single-phase shunt APF

The dynamics of the APF in Fig. 1 can be described as follows:

$$L_n \frac{di_c}{dt} = E - V_{in} \quad (1)$$

$$C_n \frac{dV_c}{dt} = S(t) i_c(t) \quad (2)$$

where the compensation current i_c and the capacitor voltage V_c are the state variables, and V_{in} is the input voltage. $S(t)$ denotes the switching function, and the value is 1 or -1. L_n and C_n are the values of the grid-side inductor and the DC link capacitor, respectively.

For the operation of the shunt APF, the grid current i_s is controlled to track the sinusoidal reference while the DC-link voltage should be kept stable. The cascaded control strategy is proposed to achieve these two control objectives. The current regulation of the shunt APF consists of two parts: One is the current control loop and the other is the reference current generator. The reference current generator is designed based on the instantaneous p - q theory, which has excellent steady-state performance and can be easily implemented^[19]. Unlike the previous current regulation methods, the DMRC and the one-sampling-ahead preview (OSAP) control integrated hybrid current regulation scheme is newly proposed for the APF. Since the focus of this paper is to investigate the performance of harmonic current tracking on the AC side, the standard PI control is used to control the DC link voltage of the APF.

2 Design and Analysis of Proposed Control Scheme

2.1 Design of OSAP controller

Eq. (1) can be described as

$$i_c(k+1) = i_c(k) + \frac{T_s}{L_n}(E(k) - V_{in}(k)) \quad (3)$$

where k and $k+1$ represent the sampling instants. The grid voltage E can be assumed constant in each sampling period T_s by considering the sampling frequency is high enough. The OSAP control algorithm is a standard deadbeat control for the current loop. It yields $i_c(k+1) = i_{ref}(k)$ with the transfer function as $H_{cl}(z) = z^{-1}$. The control law for the current-loop is given as

$$V_{in}(k) = E(k) - \frac{L_n}{T_s}(i_{ref}(k) - i_c(k)) \quad (4)$$

2.2 Proposed hybrid current control

The proposed hybrid current control scheme is shown in Fig. 2. The DMRC in the proposed hybrid controller has the controllability for both the odd and the even order harmonics. Two $N/2$ memory cells run in parallel and the controller updates its control output every $N/2$ sample intervals. Therefore, the convergence rate of the DMRC in the hybrid controller is faster than that of the conventional repetitive control schemes. The transfer function of the proposed hybrid controller is given as follows:

$$G_c(z) = ((k_o G_{ohrc}(z) + k_e G_{ehrc}(z))G_f(z) + 1)G_{osap}(z) = \left(\left(-k_o \frac{z^{-N/2}Q(z)}{1+z^{-N/2}Q(z)} + k_e \frac{z^{-N/2}Q(z)}{1-z^{-N/2}Q(z)} \right) G_f(z) + 1 \right) G_{osap}(z) \quad (5)$$

where $G_{ohrc}(z)$, $G_{ehrc}(z)$, $G_f(z) = z$ and $G_{osap}(z)$ are the discrete transfer functions of the OHRC, the even-harmonic repetitive controller (EHRC), the compensation filter and the OSAP controller, respectively. $k_o \geq 0$ and $k_e \geq 0$ are the repetitive control gains.

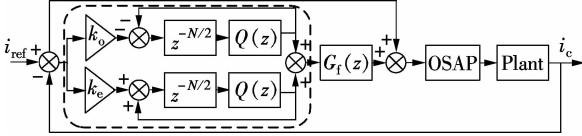


Fig. 2 Proposed hybrid current control system

In Eq. (5), a low-pass filter $Q(z)$ is employed to enhance the robustness of the system. Particularly, the DMRC will turn into an OHRC or an EHRC when $k_e = 0$ or $k_o = 0$. The DMRC can also be turned into a conventional repetitive controller (CRC) with the repetitive gain of $k_o + k_e$ when $k_o = k_e$ with the transfer function as follows:

$$-k_o \frac{z^{-N/2}}{1+z^{-N/2}} + k_e \frac{z^{-N/2}}{1-z^{-N/2}} = \frac{(k_o + k_e)z^{-N}}{1-z^{-N}} \quad (6)$$

The open-loop frequency response from $i_{ref}(z)$ to $i_c(z)$ of the hybrid current controller is given in Fig. 3. $k_o = 0.8$ and $k_e = 0.6$ are selected here as the repetitive gains. Obviously, the large gains are available at both the odd and the even order harmonics. Therefore, the proposed hybrid controller can offer a good current tracking capability for both the odd and the even order harmonics. Besides, the phase of the proposed hybrid controllers is zero at the fundamental and the harmonic frequencies by incorporating the phase compensating term $G_f(z)$. In order to enhance the robustness of the system, $Q(z) = a_0 z^{-1} + a_1 + a_0 z$ is used, where $2a_0 + a_1 = 1$. It should be mentioned that $Q(z)$ is a first-order low-pass filter with zero

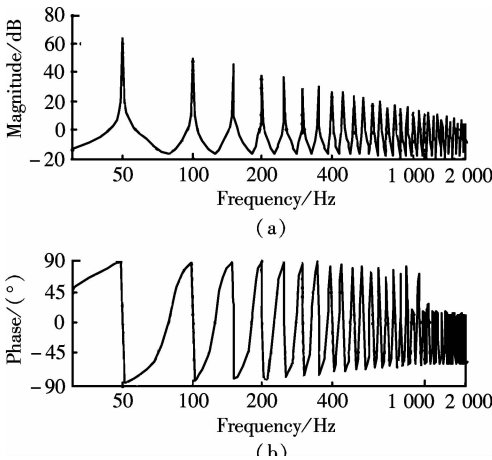


Fig. 3 Frequency response of the proposed hybrid controller. (a) Magnitude; (b) Phase

phase shift. With the increase of a_0 , the value of $\|1/Q(z)\|$ is increased, which will “push” the poles into the unit circle and make the system more stable. However, the gains beyond the cut-off frequency are reduced with the introduction of the filter. Therefore, a tradeoff design should be made between the tracking precision and the system robustness for the low-pass filter.

2.3 Analysis of voltage loop

From a physical point of view, the output of the voltage loop p_{loss} can be seen as the total loss of the APF. Therefore, the DC-link voltage is controlled to be constant in the steady state to minimize the losses, and the PI is used in the DC-link voltage controller. From Eq. (2), the DC-link voltage can be derived as

$$V_c(t) = \frac{1}{C_n} \int_{t_i}^{t_{i+1}} S(t) i_c(t) dt \quad (7)$$

Obviously, due to $S(t)$, the $V_c(t)$ in Eq. (7) is discontinuous. Eq. (7) can be averaged in one sample interval as

$$\langle V_c \rangle_{T_i} = \frac{1}{C_n} D(t) \int_{t_i}^{t_{i+1}} i_c(t) dt \quad (8)$$

where $\langle V_c \rangle_{T_i}$ represents the average value of $V_c(t)$ in a sample interval, and $D(t)$ denotes the duty ratio. Assuming that the APF is in steady-state, the compensation current i_c can be written as

$$i_c(t) = i_{cf}(t) + i_{ch}(t) = I_{cf} \sin(\omega t) + \sum_{k=1}^{\infty} I_{chk} \sin(k\omega t) \quad (9)$$

where $i_{cf}(t)$ and $i_{ch}(t)$ are the fundamental frequency and harmonic frequencies current components, respectively; ω is the fundamental frequency; and k denotes the k -th order harmonic. Considering Eq. (8) and Eq. (9), it can be found that the DC-link voltage includes not only the fundamental term but also the harmonic terms, which means both the fundamental and the harmonic components contribute to the oscillation of the DC-link voltage. Practically, only the oscillation is twice that the fundamental frequency when the power exchange between grid and APF is considered. A low-pass filter (LPF) is designed to reduce the effect of the second order harmonic. Fig. 4 shows the block diagram of the DC link voltage loop, where the measured voltage is filtered before inputting to the PI controller so that the current inner loop is less affected by the DC-link voltage variation. The cut-off frequency of the LPF is 60 Hz here. V_{dc_ref} is the reference value of the DC-link voltage.

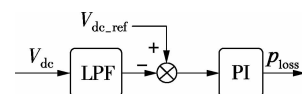


Fig. 4 Block diagram of the DC link voltage loop

2.4 Robustness analysis

In practice, the system parameter may fluctuate. The uncertainty of the system parameter can be written as

$$L_r = L_n + \Delta L \quad (10)$$

where L_r is the real values of the converter-side inductor, and ΔL is the uncertainties of the inductor. Considering the uncertainties of system parameters, the real system transfer function of $H_{cl}(z)$ becomes $H_s(z)$:

$$H_s(z) = \frac{i_c(z)}{i_{ref}(z)} = \frac{L_n}{(L_n + \Delta L)(z - 1) + L_n} \quad (11)$$

The pole map with parameter fluctuation is shown in Fig. 5. It can be seen that the pole moves from the origin point to the unity circle with the increase in $|\Delta L|$. When $\Delta L < -50\% L_n$, the pole exceeds the unit circle and the system becomes unstable. According to the stability condition of the DMRC^[17], the overall system is stable if first, the poles of $H_s(z)$ are inside the unit circle; and secondly, $0 < k_o + k_c \leq 2/(1 + \varepsilon)$. The first condition can be fulfilled when $\Delta L \geq -50\% L_n$. The second condition can be easily achieved by selecting the repetitive gains in the domain.

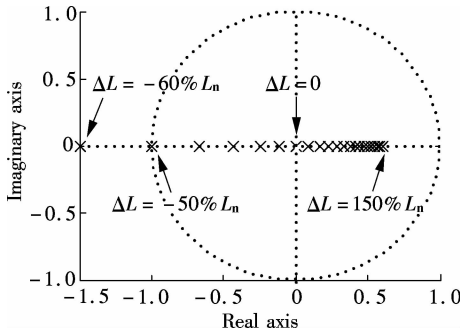


Fig. 5 Pole map of the APF system with only OSAP when the parameter fluctuates

2.5 Improvement for suppressing high order harmonics

For the frequency response of the proposed hybrid current controller in Fig. 3 (a), the gains of harmonics decrease with the increase in the harmonic order. When the harmonic frequency exceeds 1 kHz, the gains at harmonics almost approach zero. In order to eliminate some specific high order harmonics in the APF system, a modified structure of the proposed hybrid controller is proposed with the resonant controller. The zero steady-state error resonant control has been widely used in the synchronous-frame control system in recent years^[20-21]. This controller can be summarized as a set of band pass filters, which generate large gains at the selected frequency. The transfer function of resonant control for selective harmonics is illustrated as follows:

$$G_{pr} = \sum_{n=N} \frac{k_n s}{s^2 + \omega_n^2} \quad N = 1, 2, \dots \quad (12)$$

where ω_n are the selective harmonic frequencies and k_n are the control gains. The corresponding structure of the modified controller is shown in Fig. 6 (a), which incorporates both the DMRC and the resonant controller. The selective harmonic frequencies resonant controller is introduced, which aims to further reduce the selective harmonic contents. The transfer function of the modified controller is given as

$$G_m(s) = G_{dmrc}(s) + G_{pr}(s) = \underbrace{-k_o \frac{e^{-s(T_s N/2)}}{1 + e^{-s(T_s N/2)}} + k_c \frac{e^{-s(T_s N/2)}}{1 - e^{-s(T_s N/2)}}}_{\text{DMRC term}} + \underbrace{\sum_{n=N} \frac{k_n s}{s^2 + \omega_n^2}}_{\text{Resonant term}} \quad (13)$$

where $G_{dmrc}(s)$ is the transfer function of the pure DMRC. Referring to Ref. [22], the DMRC term in Eq. (13) can be derived as follows:

$$G_{dmrc} = \underbrace{-\left(k_o + \frac{k_c}{2}\right) + \frac{2k_c}{NT_s} \frac{1}{s}}_{\text{PI term}} + \underbrace{\frac{4(k_o + k_c)}{NT_s} \sum_{k=1}^{\infty} \frac{s}{s^2 + \omega_k^2}}_{\text{Resonant term}} \quad (14)$$

From Eq. (14), it can be seen that the DMRC term can be divided as a PI term and an infinite resonant term. Therefore, the differences between the pure DMRC and the modified structure controller are the control gains of the selective harmonic frequencies. The corresponding control gains change from $4(k_o + k_c)/(NT_s)$ for the pure DMRC to $4(k_o + k_c)/(NT_s) + k_n$ for the modified controller. Since k_n is not affected by the low-pass filter $Q(z)$, the magnitudes of the selective frequencies can be increased. It is noteworthy that the performance of the whole system can be improved with the increasing number of resonant units, but the computational complexity will also be increased. Fig. 6 (b) shows the open-loop frequencies response with the introduction of the 15th and

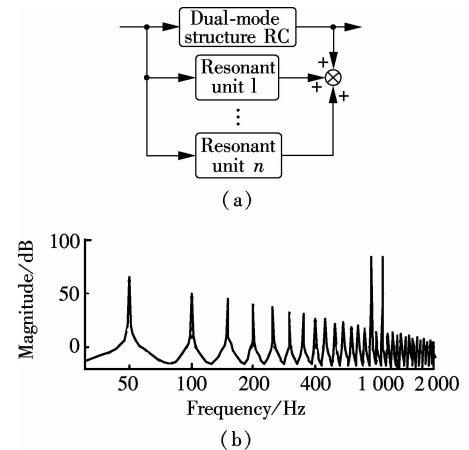


Fig. 6 Modified current controller. (a) Block diagram; (b) Open-loop frequency response

the 17th resonant units. It is obviously shown that the gains at the 15th and the 17th harmonic frequencies have been increased effectively.

2.6 Comparative analysis

The CRC-based APF^[9] and the OHRC-based APF^[14] have already been proposed to improve the power quality. Since these two methods are both internal model principle based control, the corresponding APF can track the periodic reference and reject the disturbance well. However, the shortcomings of these two control schemes for APF are also apparent.

First, the dynamic performance of the CRC-based APF is not good because of the N memory cells in the feed-forward channel. The CRC updates its output value every N sample intervals, which means that the control signal will be updated in at least one fundamental cycle. Secondly, the even-harmonic suppression ability of the OHRC-based APF is weak. Since the OHRC is designed only for the odd-harmonic frequency, the even-harmonic can hardly be eliminated by this type of the APF. Therefore, the steady-state performance of the OHRC-based APF is limited. The hybrid control scheme proposed in this paper overcomes the shortcomings of the two methods and achieves good steady-state and dynamic performance.

From Refs. [22] and [23], it can be concluded that the CRC and the DMRC have the controllability for DC component, the fundamental component and different order harmonics, while the OHRC can only track for the fundamental component and the odd harmonic signals. For the fundamental and odd-harmonic signals, the tracking performance of the OHRC is better than that of the CRC when the same repetitive gains are employed, namely, $k_o = k_r$ (k_r is the repetitive gain of the CRC). This is due to the fact that the equivalent odd-harmonic resonant gains of the OHRC are twice larger than those of the CRC. Meanwhile, the equivalent resonant gains of the DMRC is larger than those of the CRC for all the interesting frequencies when $k_o + k_e = k_r$. The stability domain of repetitive gain k_r for the CRC is $0 < k_r \leq 2/(1 + \varepsilon)$, which is the same as the stability domain of $k_o + k_e$ ^[9]. Therefore, compared with the CRC scheme, the DMRC can achieve better tracking performance for both the fundamental and the harmonic components. Moreover, the two repetitive gains k_o and k_e can be adjusted separately to fulfill the requirement of compensation of different harmonic contents under different conditions.

3 Experimental Verification

To verify the proposed hybrid current regulation scheme experimentally, the laboratory setup is built and the experiments are carried out. The experimental prototype of the APF is based on a Semikron AN-8005 (an H-bridge IGBT inverter). The system configuration is the

same as the system configuration described in Fig. 1. The single-phase shunt APF is controlled using a dSPACE DS1104 controller card. The parameters are selected as follows: $V_c = 100$ V, $E = 65$ V, $L_n = 5$ mH, $C_n = 5\,500$ μ F, $f = 50$ Hz, $L_{ac} = 3$ mH, and the switching frequency $f_s = 10$ kHz. The nonlinear load is a full-wave diode rectifier with $C_r = 2\,200$ μ F. The reactive power with the nominal resistor is approximately zero.

First, Fig. 7(a) shows the grid current with OSAP + CRC; Fig. 7(b) shows the grid current of OSAP + OHRC; and Fig. 7(c) shows the grid current of the hybrid current controller. Fig. 8 shows the measured harmonic spectrum of the three schemes. It is observed that the total harmonic distortion (THD) values are 5.88% and 4.63% for OSAP + CRC and OSAP + OHRC, respectively. The value is reduced to 3.35% by using the proposed hybrid controller. Compared with the CRC approach, the steady-state performance is better and the harmonic contents are lower for almost all the interesting

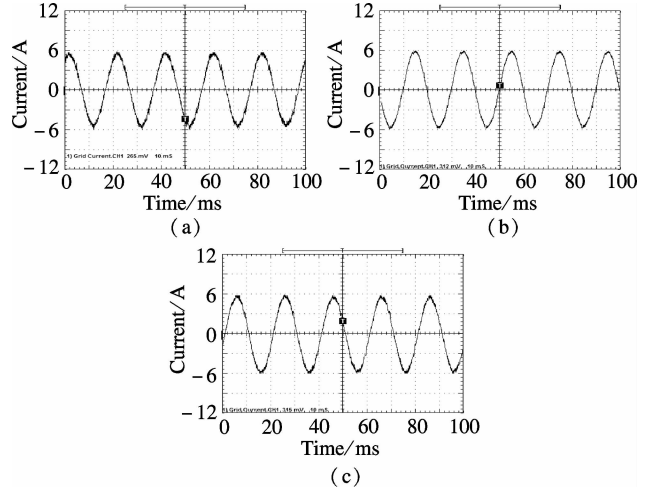


Fig. 7 Grid current waveform after compensation. (a) OSAP + CRC-controlled APF; (b) OSAP + OHRC-controlled APF; (c) Proposed hybrid-controlled APF

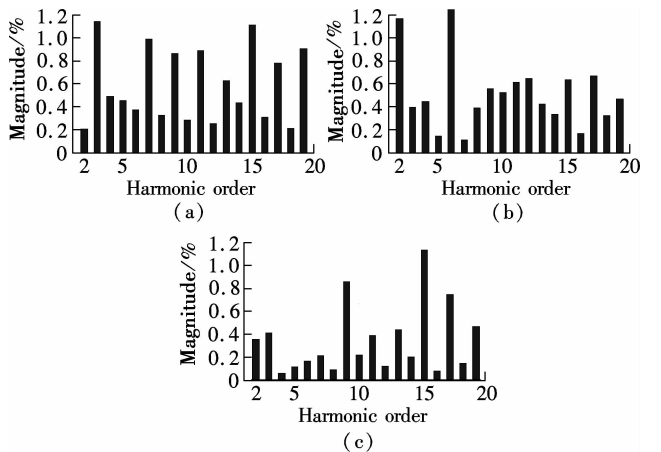


Fig. 8 Harmonic content of grid current. (a) OSAP + CRC-controlled APF; (b) OSAP + OHRC-controlled APF; (c) Proposed hybrid-controlled APF

frequencies. Compared with the OHRC approach, the proposed DMRC-based hybrid controller has superiority in compensation ability since it can suppress not only the odd order but also the even order harmonics.

Secondly, Fig. 9 shows the measured transient tracking performance of the compensation current with the OSAP + CRC, the OSAP + OHRC, and the proposed hybrid control. In Fig. 9(a), the OSAP + CRC starts working at $t = 0.4$ s. The tracking error between the reference current and the real current is reduced from 2 to 0.3 A, and the convergence time is about 1 s. In Fig. 9(b), the OSAP + OHRC controller works at $t = 0.4$ s. The corresponding tracking error is reduced from 3 to 0.3 A, and the convergence time is about 0.6 s. In Fig. 9(c), the hybrid controller begins to work at the same time, and the transient effect is almost the same as that of Fig. 9(b). It is obvious that the OSAP + OHRC controller and the proposed hybrid controller have a better convergence rate compared with the OSAP + CRC controller.

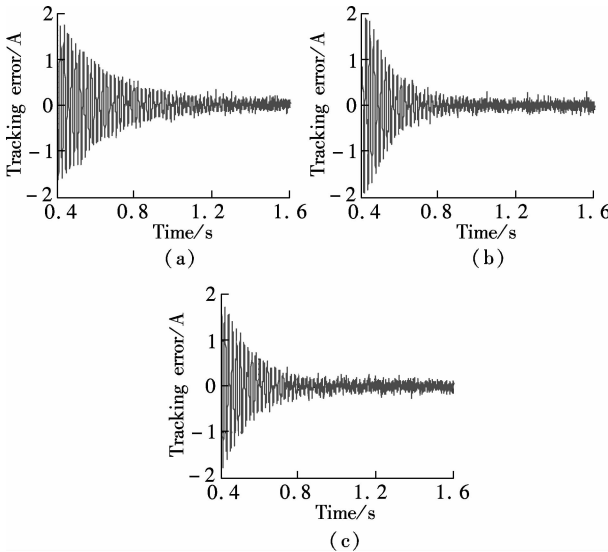


Fig. 9 Tracking error of the compensation current. (a) OSAP + CRC-controlled APF; (b) OSAP + OHRC-controlled APF; (c) The proposed hybrid-controlled APF

Finally, Fig. 10(a) and Fig. 10(b) show the measured grid current with the compensation of the proposed hybrid controller plus the 15th and the 17th order resonant units and the corresponding harmonic content. Compared with Fig. 9(c), it is obviously seen that the contents of the

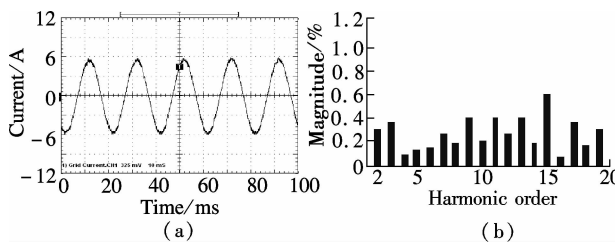


Fig. 10 Measured grid current using the proposed hybrid controller plus 15th and 17th order resonant units. (a) Grid current; (b) Harmonic contents

15th and the 17th order harmonics have been reduced effectively. The THD of the grid current is further suppressed with the introduction of resonant units, and the value is 2.23%.

4 Conclusion

In this paper, a novel hybrid current regulation scheme is proposed for the single-phase shunt APF by integrating the deadbeat control and the DMRC. The all-digital approach can be easily implemented and can also be extended into a three-phase APF system. It not only offers better tracking ability for current harmonics compensation, but also maintains good transient performance. This paper also presents a modified structure, which incorporates the proposed hybrid current controller and the resonant controller, to further suppress some high order specific harmonics. As analyzed in this paper, the DMRC can be regarded as a set of resonant controllers plus a PI term. With the integration of the DMRC and the selective harmonic resonant controller, the control gain at the selective harmonic frequency can be adjusted flexibly. Additionally, the relationships among different repetitive control schemes are also shown. By the experimental results, it is verified that the THD performance of the proposed hybrid controller is better than that of the OHRC + OSAP approach, and its transient performance is better than that of the CRC + OSAP approach. The grid current can achieve good performance and meet the requirements of IEEE 519 quite well.

References

- [1] Akagi H. Trends in active power line conditioners [J]. *IEEE Trans Power Electronics*, 1994, **9**(5): 263–268.
- [2] Fujita H, Akagi H. A practical approach to harmonic compensation in power systems-series connection of passive and active filters [J]. *IEEE Trans Industry Applications*, 1991, **27**(6): 1020–1025.
- [3] Green T C, Marks J H. Control techniques for active power filters [J]. *IEE Proceedings of Electric Power Applications*, 2005, **152**(2): 369–381.
- [4] Singh B, Al-Haddad K, Chandra A. A review of active filters for power quality improvement [J]. *IEEE Trans Industrial Electronics*, 1999, **46**(5): 960–971.
- [5] Buso S, Malesani L, Mattavelli P. Comparison of current control techniques for active filter applications [J]. *IEEE Trans Industrial Electronics*, 1998, **45**(5): 722–729.
- [6] Lin B R, Tsay S C, Liao M S. Integrated power factor compensator based on sliding mode controller [J]. *IEE Proceedings of Electric Power Applications*, 2001, **148**(3): 237–244.
- [7] Nishida K, Rukonuzzman M, Nakaoka M. Advanced current control implementation with robust deadbeat algorithm for shunt single-phase voltage-source type active power filter [J]. *IEE Proceedings of Electric Power Applications*, 2004, **151**(3): 283–288.
- [8] Teodorescu R, Liserre M, Rodríguez P. *Grid converters*

- for photovoltaic and wind power systems [M]. New Jersey: Wiley, 2011:289–311.
- [9] Garcia-Cerrada A, Pinzon-Ardila O, Feliu-Batlle V, et al. Application of a repetitive controller for a three-phase active power filter [J]. *IEEE Trans Power Electronics*, 2007, **22**(1): 237–246.
- [10] Escobar G, Hernandez-Briones P G, Martinez P R, et al. A repetitive-based controller for the compensation of $6l \pm 1$ harmonic components [J]. *IEEE Trans Industrial Electronics*, 2008, **55**(4): 3150–3158.
- [11] Costa-Castelló R, Grino R, Parpal R C, et al. High-performance control of a single-phase shunt active filter [J]. *IEEE Trans Control Systems Technology*, 2009, **17**(6): 1318–1329.
- [12] Ramos G A, Costa-Castelló R. Power factor correction and harmonic compensation using second-order odd-harmonic repetitive control [J]. *IET Control Theory & Applications*, 2012, **6**(11): 1633–1644.
- [13] Grino R, Costa-Castelló R. Digital repetitive plug-in controller for odd-harmonic periodic references and disturbances [J]. *Automatica*, 2005, **41**(1): 153–157.
- [14] Costa-Castelló R, Grino R, Fossas E. Odd-harmonic digital repetitive control of a single-phase current active filter [J]. *IEEE Trans Power Electronics*, 2004, **19**(1): 1060–1068.
- [15] Buddingh P C. Even harmonic resonance-an unusual problem [J]. *IEEE Trans Industry Applications*, 2003, **39**(1): 1181–1186.
- [16] Taylor J B. Even harmonics in alternating-current circuits [J]. *Transactions of the American Institute of Electrical Engineers*, 1909, **XXV**(1): 725–732.
- [17] Zhou K, Wang D, Zhang B, et al. Dual-mode structure digital repetitive control [J]. *Automatica*, 2007, **43**(3): 546–554.
- [18] Cosner C, Anwar G, Tomizuka M. Plug in repetitive control for industrial robotic manipulators [C]//*Proc IEEE Int Conf Robot Automat*. Cincinnati, OH, USA, 1990:1970–1975.
- [19] Superti-Furga G, Todeschini G. Discussion on instantaneous p-q strategies for control of active filters [J]. *IEEE Trans Power Electronics*, 2008, **23**(7): 1945–1955.
- [20] Liserre M, Teodorescu R, Blaabjerg F. Multiple harmonics control for three-phase grid converter systems with the use of PI-RES current controller in a rotating frame [J]. *IEEE Trans Power Electronics*, 2006, **21**(5): 836–841.
- [21] Lascu C, Asiminoaei L, Boldea I, et al. High performance current controller for selective harmonic compensation in active power filters [J]. *IEEE Trans Power Electronics*, 2007, **22**(9): 1826–1835.
- [22] Zou Z, Wang Z, Cheng M. Design and analysis of operating strategies for a generalised voltage-source power supply based on internal model principle [J/OL]. *IET Power Electronics*. (2013-08-21) [2013-10-09]. <http://digital-library.theiet.org/content/journals/10.1049/iet-pel.2013.0159>.
- [23] Zou Z, Wang Z, Cheng M. Modeling, analysis, and design of multi-function grid-interfaced inverters with output LCL filter [J/OL]. *IEEE Trans Power Electronics*. (2013-09-04) [2013-10-09]. http://ieeexplore.ieee.org/xpls/abs_all.jsp?arnumber=6588968&tag=1.

基于双模结构重复控制器的有源电力滤波器 混合电流控制方案的设计与分析

邹志翔 王 政 程 明

(东南大学电气工程学院, 南京 210096)

摘要:提出了一种用于单相有源电力滤波器的全数字式混合电流控制方案. 该混合电流控制方案结合无差拍控制以及双模结构重复控制以实现优异的稳态性能和动态特性. 区别于传统方案, 采用该方案的有源电力滤波器可消除电网中存在的奇次和偶次谐波. 给出了该混合电流控制方案的详细设计原则, 并进行了稳定性分析. 在此基础上, 提出了混合电流控制结合谐振控制器的一种优选方案以消除电网中的特定次谐波, 并讨论了谐振控制与几种重复控制的内在联系. 实验结果验证了电流控制方案在有源电力滤波器中的优点和有效性.

关键词:有源电力滤波器; 双模结构重复控制器; 电流控制; 谐波补偿; 谐振控制器

中图分类号:TM53